ACS SyntheticBiology

Research Article

pubs.acs.org/synthbio

Improving the Gene-Regulation Ability of Small RNAs by Scaffold Engineering in *Escherichia coli*

Yuta Sakai,[†,‡] Koichi Abe,[†,‡] Saki Nakashima,[†,‡] Wataru Yoshida,[†,‡,§] Stefano Ferri,[†,‡] Koji Sode,[†,‡] and Kazunori Ikebukuro*[,†,‡]

[†]Department of Biotechnology and Life Science, Graduate School of Engineering, Tokyo University of Agriculture and Technology, 2-24-16 Naka-cho, Koganei, Tokyo 184-8588, Japan

[‡]Japan Science and Technology Agency, CREST, 2-24-16 Naka-cho, Koganei, Tokyo 184-8588, Japan

Supporting Information

ABSTRACT: Noncoding small RNAs are involved in transcriptional and post-transcriptional gene regulation of target mRNAs by modulating mRNA elongation, stability, or translational efficiency. Many natural *trans*-encoded small RNAs contain a scaffold that allows binding of the RNA chaperone protein Hfq for conditional gene regulation. Here, we improved the gene regulation abilities of small RNAs by directly fusing the natural *Escherichia coli trans*-encoded small RNA-derived scaffolds, including Hfq-binding and rho-independent transcription terminator sequences, to the 3′ end of the small RNAs that mediate RNA-based gene regulation. As target small RNAs to improve their gene regulation abilities, we selected small RNAs of artificial post-transcriptional riboregulators and transcriptional attenuators. Four different small RNA scaffolds were fused to the riboregulator and attenuator-derived small RNAs. Mutations were introduced into the best small RNA scaffold to improve its gene-regulation ability further. As a result, mutations predicted to stabilize the secondary structures of the small RNA scaffolds dramatically increased its ability to regulate gene expression of both the post-transcriptional riboregulator and transcriptional attenuator systems. We believe our engineered small RNA scaffolds are applicable to other RNA regulators for improving regulatory activity, and engineered small RNA scaffolds may present a valuable strategy to regulate target gene expression strongly.

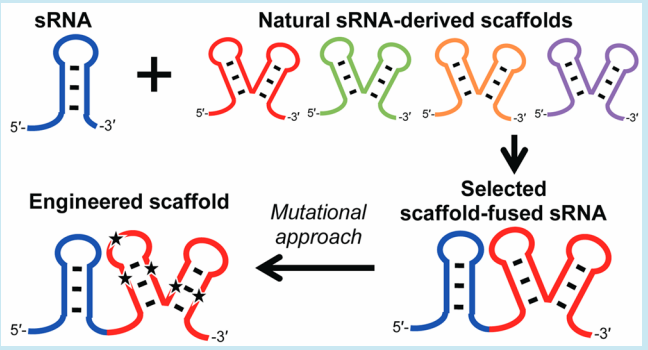

KEYWORDS: *attenuator, Hfq, post-transcriptional gene regulation, riboregulator, small RNA, transcriptional gene regulation*

In synthetic biology, the design of genetic tools is important because appropriate gene regulation is critical to the implementation of designed multigene circuits. It is important to control the expression levels of individual genes to operate genetic circuits at desired levels and to achieve idealized dynamic ranges, particularly when regulating toxic genes or those that may interfere with the host machinery.[1−3] Such optimization of gene expression can improve the functional efficiency of genetic circuits to design precise logic gates as well as the high-yield production of biofuel-related compounds by incorporating regulators that sense intermediates of the metabolic and/or biosynthetic pathways.[3−6] To date, diverse gene regulators have been designed, such as constitutive, inducible promoters with high dynamic ranges,[7−9] libraries of ribosomal binding sites (RBSs),[1,5] and RNA-based regulators that respond to specific ligands or target specific genes.[10−23]

Noncoding small RNAs (sRNAs) are naturally occurring molecules that transcriptionally and post-transcriptionally regulate gene expression to control cellular processes in response to extracellular stress.[24,25] To date, many naturally occurring sRNAs have already been identified and characterized in diverse organisms, particularly in *Escherichia coli*.[26−28] sRNAs regulate their respective target gene by base pairing with the 5′ untranslated region (UTR), mRNA coding region, or the 3′ UTR, thereby modulating mRNA elongation, stability, or translational efficiency, resulting in the activation or repression of gene expression.[24,25,29−34] This gene-regulation mechanism based on RNA−RNA hybridization allows RNA gene regulators to be tunable by modulating the duplex length and introducing mismatched base pairs.[11]

RNA-based regulators, such as artificial sRNAs and antisense RNAs, can be designed on the basis of the complementary sequence of their target mRNA sequences. To date, chimeric sRNAs, designed by fusing two individual sRNAs, have demonstrated the ability to regulate target gene expression in a similar fashion to naturally occurring sRNAs. Owing to their ease of design and gene-regulation abilities, RNA-based regulators have been described as efficient artificial gene regulators of target gene expression.[35] Recently, the engineering

Special Issue: SB6.0

Received: July 31, 2013
Published: December 11, 2013

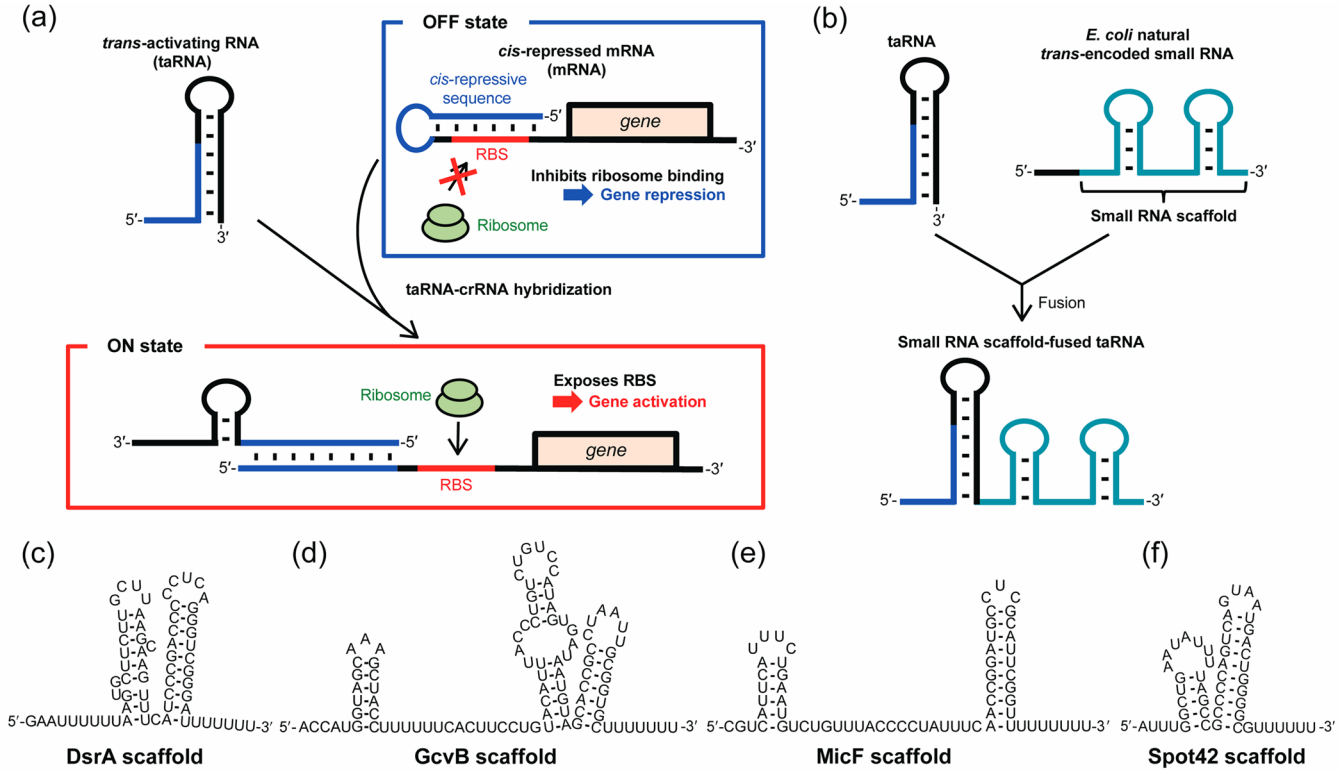

Figure 1. Target gene regulation mediated by taRNA and the fusion of an sRNA scaffold. (a) taRNA hybridized with the crRNA *cis*-repressive sequence, which formed a hairpin structure to block ribosome binding and exposed the RBS, resulting in gene activation. (b) sRNA scaffolds were directly fused to the 3′ end of taRNA of the riboregulator system. The selected sRNA scaffolds from (c) DsrA, (d) GcvB, (e) MicF, and (f) Spot42 contain a Hfq-binding sequence and a rho-independent transcription terminator.

of target-specific artificial sRNAs inspired by naturally occurring *trans*-encoded sRNAs have been reported.[17,19−21] These engineered artificial sRNAs harbor an sRNA scaffold containing an Hfq-binding sequence and rho-independent transcription terminator sequence. These scaffolds are derived from endogenous *E. coli trans*-encoded sRNAs located at different genomic locations from the mRNAs that they regulate. Hfq is an RNA chaperone protein that is commonly required for gene regulation by *trans*-encoded sRNAs.[27,36−39] Hfq binds to a single-stranded AU-rich sequence outside of the antisense region that hybridizes to the mRNA and promotes sRNA−mRNA hybridization and also enhances the stability of sRNAs by protecting from ribonuclease degradation.[29,36,37,40,41] Artificial sRNAs have been engineered by screening functional antisense sequences from an artificial sRNA library that are composed of randomized antisense regions fused to sRNA scaffolds.[19,20] Another approach was to select a combination of Hfq-binding sequences and rho-independent transcription terminators based on M-fold prediction[42] that are suitable for the artificial antisense sequence complementary to target mRNA[17] or by directly fusing the sRNA scaffolds to the designed antisense sequences to regulate a biosynthetic pathway.[21]

An important goal is to engineer sRNAs that provide strong gene-regulation capabilities to control genetic circuits better. However, considering that sRNA-mediated gene regulation is dependent on the length and strength of the sRNA−mRNA hybrid or on the secondary structure of the target mRNAs, a conventional strategy to improve sRNA-associated gene regulation is to elongate the antisense sequence or to target different sequence regions,[21] although altering antisense regions may affect the specificity of sRNA against target sequences and create crosstalk.[19] Moreover, a newly engineered sRNA may not promote gene regulation. Therefore, an alternative strategy to improve sRNA gene regulation is required and will be even more valuable if the engineering strategy can be applied to improve a wide range of sRNAs that regulate target gene expression by different mechanisms.

Although the antisense regions of natural and artificial sRNAs have been characterized, the sRNA scaffolds remain potential targets to improve sRNA-mediated gene regulation. In the present study, to improve sRNAs gene-regulation abilities, we focused on the engineering of the scaffold regions, which are directly fused to sRNAs that act as (i) post-transcriptional gene regulators (riboregulators)[2,10−13] and (ii) transcriptional gene regulators (attenuators).[14−16] Riboregulators and attenuators regulate gene expression by different mechanisms and have been described as valuable genetic tools in several synthetic-biology applications.[10,14,15] The sRNA scaffolds containing the Hfq-binding sequence and rho-independent transcription terminator were derived from naturally occurring *E. coli* Hfq-dependent sRNAs.[19] The gene-regulation abilities of sRNA scaffold-fused gene regulators were enhanced by a rational mutation approach to stabilize their predicted secondary structures and by introducing sequences with high affinities to Hfq, based on M-fold secondary-structure prediction.[42] These mutational approach were also tested against a natural *E. coli*-derived *trans*-encoded MicF sRNA.[43]

RESULTS AND DISCUSSION

Fusion of *Escherichia coli Trans*-Encoded Small-RNA-Derived Scaffolds to Artificial Riboregulators. As a target

dx.doi.org/10.1021/sb4000959 | *ACS Synth. Biol.* 2014, 3, 152−162

sRNA-based gene regulator, we selected an artificial riboregulator, which is a gene regulatory system that activates target gene expression through sRNA−mRNA hybridization, to improve its gene regulation further.[2,10−13] Riboregulator is composed of two RNA molecules: *cis*-repressed mRNA (crRNA) and *trans*-activating noncoding sRNA (taRNA) (Figure 1a). The crRNA contains a sequence complementary to the RBS and forms a hairpin structure in its 5′ UTR to prevent ribosomal binding, thereby repressing expression of the target gene, whereas taRNA hybridizes with the crRNA through a linear−loop interaction that exposes the RBS by dissociating from the crRNA hairpin structure and subsequently activating post-transcriptional expression of the target gene. The application of riboregulators has been described as a proficient gene-regulatory method through the regulation of toxic genes expression[2] and metabolic pathways.[11] However, the expression efficiency of the riboregulator system was approximately 10% of that of a promoter-mediated transcriptional regulatory system.[10] If gene expression of a riboregulator system can be enhanced in the presence of taRNA without varying the expression level in its absence, then the riboregulator will be a stronger genetic tool available for additional applications such as the design of genetic circuits requiring high expression.

Both taRNA and crRNA were designed on the basis of the natural *hok*/*sok* gene-regulatory system of plasmid R1.[44] Sok is a *cis*-encoded sRNA that does not require Hfq-binding. Therefore, taRNA does not contain an sRNA scaffold harboring the Hfq-binding sequence. To enhance the riboregulator expression level in the presence of taRNA, we directly fused sRNA scaffolds. Four different sRNA scaffolds derived from natural *E. coli trans*-encoded sRNAs[30,43,45,46] (DsrA, GcvB, MicF, and Spot42) were selected to be fused to the 3′ end of taR12, which was previously designed by Isaacs et al. (Figure 1b−f and Supporting Information Figure S1).[10] We selected these four sRNAs because they were known to interact with Hfq *in vitro* and because it has been demonstrated that Hfq is required for the target-gene-regulation abilities of each *in vivo*.[27,29,36,37,39,41] In addition, these sRNAs were previously selected as scaffolds for screening artificial sRNAs against target genes.[19] Each sRNA-scaffold-fused taR12 was evaluated by transcription under arabinose-inducible promoter P_{araBAD} on the high-copy-plasmid pSB1K3. The taR12s harboring different sRNA scaffolds were evaluated by measuring GFPuv expression levels (Figure 2a). Three scaffold fusions (taR12-DsrA, taR12-MicF, and taR12-Spot42) increased the expression level compared with taR12 alone. The greatest increase was observed with taR12-MicF, which exhibited a 28-fold increase in GFPuv expression, 2.7-fold higher than that of taR12. The four sRNA-scaffold-fused taR12s were evaluated in an *hfq* deletion strain[47] (provided courtesy of Dr. Hiroji Aiba) to determine whether the sRNA-scaffold-fused taR12s require *hfq* for gene regulation. Because this strain (*E. coli* K-12 W3110 Δ*hfq*) and the host strain (*E. coli* K-12 W3110) metabolize arabinose, the arabinose-inducible P_{araBAD} promoter was substituted with the $P_{LtetO-1}$ promoter, which acts as a constitutive promoter in our system. All taR12s exhibited similar cellular fluorescence in the Δ*hfq* strain, similar to the natural *trans*-encoded sRNAs reported previously[39,41] (Figure 2b). Meanwhile, the taR12s exhibited a lower fold expression in the Δ*hfq* strain, which may be due to the difference in the intracellular environment. However, these results demonstrated that the sRNA-scaffold-fused taR12s were Hfq-dependent and require Hfq to induce higher gene expression than taR12 as well as natural *trans*-encoded sRNAs.

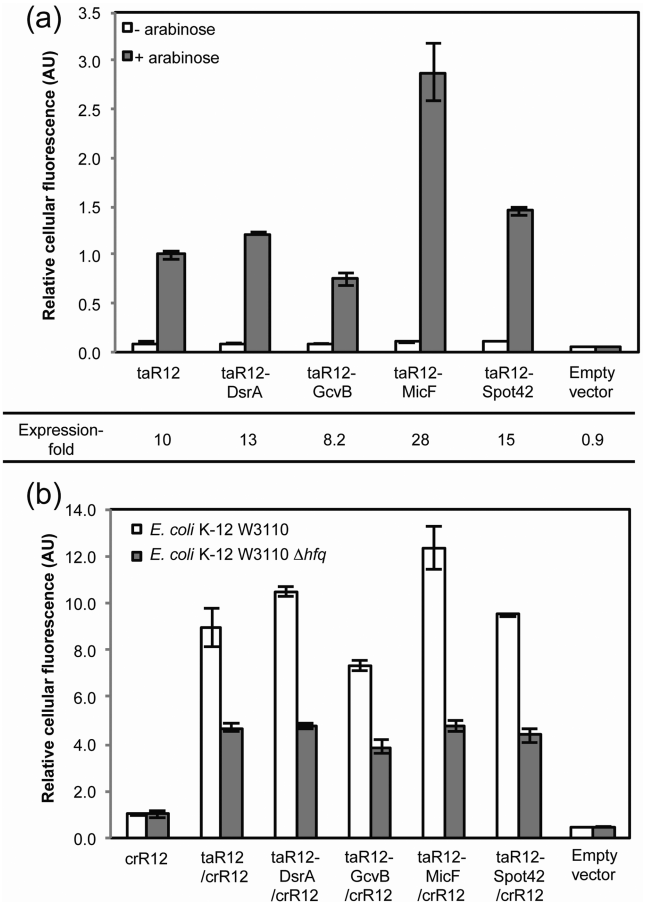

Figure 2. Small RNA-scaffold-fused taR12. (a) taR12 transcription was regulated using arabinose-inducible promoter P_{araBAD} and evaluated by measuring the increase in cellular fluorescence when inducing transcription by adding L-arabinose. The cellular fluorescence of taR12 in the presence of L-arabinose was normalized to 1.0. The expression fold representing the ratio of GFPuv expression levels in the presence and absence of L-arabinose are shown. (b) Evaluation of scaffold-fused taR12s in the *E. coli* K-12 W3110 and Δ*hfq* strains (*E. coli* K-12 W3110 Δ*hfq*). The taR12s were transcribed constitutively by $P_{LtetO-1}$. The cellular fluorescence of crR12 was normalized to 1.0. The graphs depict the mean and error bars represent the standard deviation of experiments performed in triplicate.

Fusion of the MicF scaffold may stabilize the structure of taR12 to allow taR12−crR12 hybridization through a linear−loop interaction, which is considered to be critical to activate gene expression of the riboregulator. In contrast, taR12-GcvB decreased the induction level compared with taR12, probably because of an intramolecular interaction between the GcvB scaffold and the antisense region of taR12, as predicted by M-fold analysis (Supporting Information Figure S4). Fusion of the above sRNA scaffolds to taR*2, an additional taRNA that we engineered,[13] demonstrated similar results (Supporting Information Figures S2 and S5). The fusion of DsrA, MicF, and Spot42 sRNA scaffolds to taR*2 increased the induction level, whereas fusion of the GcvB scaffold exhibited a similar fold expression as taR*2. Moreover, taR*2-MicF exhibited the highest expression increase, which was 2.2-fold higher than that of taR*2 without an sRNA scaffold.

dx.doi.org/10.1021/sb4000959 | *ACS Synth. Biol.* 2014, 3, 152−162

Effects of Single-Stranded AU-Rich Sequences in MicF Scaffold. To engineer powerful RNA-based gene regulators further, we sought to improve the gene-regulatory abilities of taRNA-MicF. The conventional strategy to improve sRNA gene regulation is to engineer the antisense region for prolonged hybridization or by targeting different sequence regions.[21] However, altering the antisense regions may affect the specificity of the sRNA. Therefore, we focused on the scaffold region to improve sRNA-mediated gene regulation by introducing mutations. To determine an appropriate target MicF scaffold region suitable for mutation, we first focused on the single-stranded AU-rich sequences present in the loop region of the upstream hairpin and between the two hairpins structures. Hfq binding primarily occurs within the single-stranded AU-rich sequences of Hfq-dependent *E. coli* sRNAs,[29,36,38,41] and it was previously shown that Hfq binds to MicF sRNA,[27] although the exact Hfq-binding sequence has not yet been reported. To examine whether we could introduce mutations into the single-stranded AU-rich sequences, they were substituted with GC-rich sequences to design four variants, M1.1−M1.4 (Figure 3a). These variants were designed on the basis of M-fold prediction to ensure that the most stable predicted secondary structures were not altered. The variants were tested and shown to exhibit decreased expression compared to taR12-MicF (Figure 3b), particularly by the deletion or substitution of the single-stranded AU-sequences present between the two hairpin structures with GC-sequence, which resulted in an average 30% decrease in GFPuv expression by the taR12-MicF M1.2, M1.3, and M1.4 variants, indicating the single-stranded AU-sequence present between the two hairpin structures is involved in taRNA-MicF gene activation. This sequence substitution also decreased the fold expression of taR*2-MicF (Supporting Information Figure S6). However, the sequence substitution within the loop region of the upstream hairpin did not decrease the fold expression as it did in the linear region, which was probably because of the effect of Hfq binding, as Hfq prefers to bind to single-stranded AU-rich sequences.[29,36,38,41] This result indicated that the single-stranded AU-rich sequences between the two hairpins should be intact.

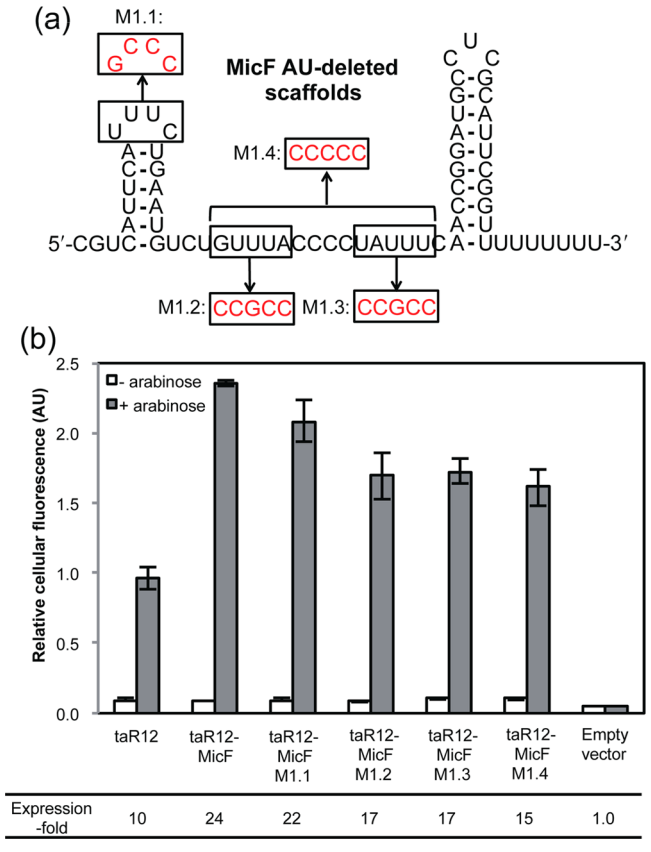

Figure 3. Effect of the AU-rich sequence of MicF-scaffold-fused taR12. (a) Four variants (M1.1−M1.4) were designed, and the single-stranded AU-rich sequences were deleted or substituted with GC-rich sequences (red). (b) Cellular fluorescence in the presence of taR12 and taR12-MicFs. The cellular fluorescence of taR12 in the presence of L-arabinose was normalized to 1.0. The fold expression representing the ratio of GFPuv expression levels in the presence and absence of L-arabinose is shown. The graphs depict the mean and error bars represent the standard deviation of experiments performed in triplicate.

Improving taRNA-MicF Fold Expression by Stabilization of the Hairpin Structures and Introduction of a Sequence with High Affinity to Hfq. Deletion of the single-stranded AU-rich sequences present in the MicF scaffold decreased the gene-regulation abilities of the taRNAs, indicating that they may play a functional role. Therefore, to improve the gene-regulation abilities further, we introduced additional AU-rich sequences into the MicF scaffold. We designed the M2.1−M2.3 variants (Supporting Information Figure S7) in which the GC-sequences present between the two hairpin structures of the MicF scaffold were substituted with (AU-rich) sequences that were reported to have high affinity to Hfq *in vitro*.[48,49] These variants were also designed using M-fold analysis to ensure that the secondary structures remained unaltered. However, none of the taR12/taR*2-MicF variants showed enhanced induction levels (Supporting Information Figures S8 and S9).

The main reason for the observed decrease in the induction level by taR12 when fused with the GcvB scaffold was predicted by M-fold analysis to be the intramolecular interaction between the antisense region of taR12 and the GcvB scaffold. However, fusion with the DsrA, MicF, and Spot42 sRNA scaffolds probably enabled Hfq binding and also may have stabilized the secondary structure of taR12 to increase the amount that can interact with crR12 to induce gene expression. Taking this into consideration, we introduced mutations predicted to stabilize the secondary structure of the MicF scaffold to increase the gene-expression level further. AU and GU base pairs located in the upstream and downstream hairpins were substituted with GC base pairs (Figure 4a). The substitution in either the upstream (M3.1) or downstream (M3.2) hairpin sequence slightly increased the induction level, whereas the substitutions in both hairpins (M4.3) resulted in a smaller increase (Figure 4b). When the upstream loop sequence 5′-UUUC-3′ in taR12-MicF M4.3 was substituted with the Hfq high-affinity sequence 5′-AGGA-3′,[49] a 46-fold induction level was observed, 1.9-fold and 5.1-fold higher than taR12-MicF and taR12, respectively. However, substituting only the loop sequence (MicF M6.4 scaffold) did not increase the expression level (Supporting Information Figures S8 and S9). The improvement observed with taR12-MicF M7.4 may be due to the optimization of the loop sequence of the MicF scaffold harboring stabilized hairpins, whereas the newly formed loop sequence did not increase gene expression of taR12-MicF M6.4. Similar increases in expression levels were observed when these mutations were applied to taR*2 (Supporting Information Figure S9).

dx.doi.org/10.1021/sb4000959 | *ACS Synth. Biol.* 2014, 3, 152−162

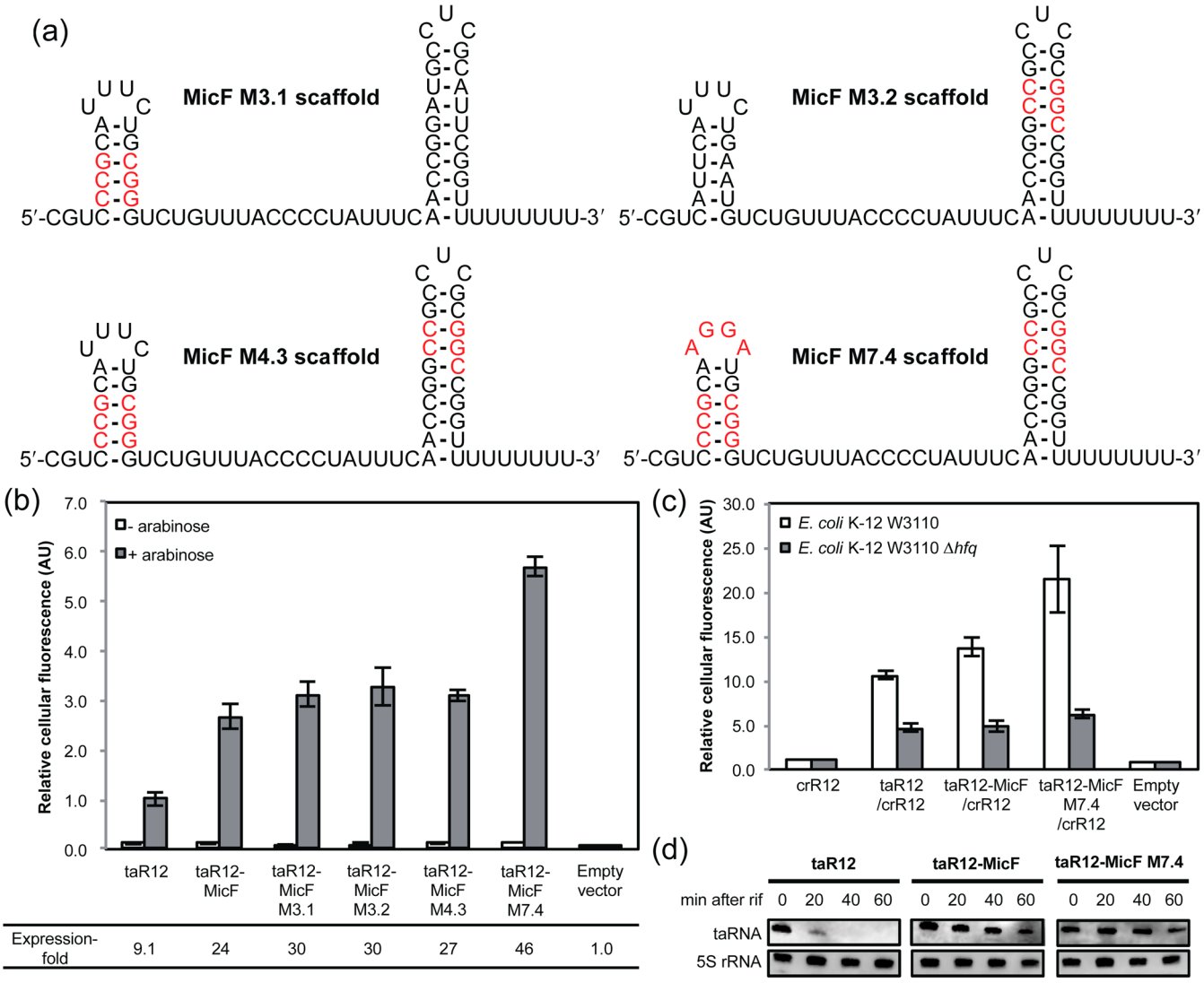

Figure 4. Improvements in taR12-MicF by introducing mutations. (a) Against the upstream hairpin, downstream hairpin, and loop region, mutations (red) predicted to stabilize the secondary structures and sequences that showed high affinity to Hfq were introduced. (b) Cellular fluorescence in the presence of taR12 and taR12-MicFs. The fold expression representing the ratio of GFPuv expression level in the presence and absence of L-arabinose is shown. The cellular fluorescence of taR12 in the presence of L-arabinose was normalized to 1.0. (c) Cellular fluorescence of taR12 and taR12-MicFs compared to crR12 and evaluated in the *E. coli* K-12 W3110 and Δ*hfq* strains (*E. coli* K-12 W3110 Δ*hfq*). The cellular fluorescence of crR12 was normalized to 1.0. (d) Northern blot analysis of taR12 and taR12-MicFs stability. The strains were grown overnight at 37 °C in the presence of 0.1% L-arabinose. After incubation, rifampicin was added, and cells were harvested at the indicated time points for RNA preparation. Total RNA was analyzed using probes specific for taR12 and 5S rRNA, respectively. The graphs depict the mean and error bars represent the standard deviation of experiments performed in triplicate.

Moreover, the taR12/taR*2-MicF harboring the M7.4 mutation did not activate gene expression higher than taR12 or taR*2 without the sRNA scaffold in the Δ*hfq* strain (Figure 4c and Supporting Information Figure S10). Next, we performed northern blot analysis to evaluate the stabilities of taR12-MicF and taR12-MicF M7.4, which revealed that both were more stable and had longer half-lives than taR12 (Figure 4d). The binding of Hfq stabilizes natural *trans*-encoded sRNAs by protecting them from RNase E degradation.[29,36] Our observations indicated that Hfq binds to the scaffold-fused taRNAs and enhances their stabilities, thereby resulting in increased gene-regulation abilities.

Furthermore, we compared the gene-expression efficiencies of taR12, taR12-MicF, and taR12-MicF M7.4 with a transcriptional gene regulator in which GFPuv expression was controlled by the P_{araBAD} promoter. To achieve a similar transcription level, taR12s and crR12 were regulated together under the control of P_{araBAD} on the same high-copy-number plasmid pSB1K3. The GFPuv expression level was normalized with the values in the absence of L-arabinose. Compared to GFPuv expression controlled by the P_{araBAD} promoter, the expression level with taR12-MicF M7.4/crR12 was 40%, whereas that with taR12/crR12 was 13% (Supporting Information Figure S11). This result suggested that taR12-MicF M7.4 can activate approximately 40% of the crR12 transcripts.

Our results suggested that the avoidance of intramolecular interactions between the antisense region and the sRNA scaffold is one criterion to evade complications when applying our strategy. When we fused the GcvB scaffold to taR12, the resulting taR12-GcvB exhibited decreased expression ability compared with taR12 without the scaffold (Figure 2a). Intramolecular interaction was predicted by M-fold analysis

dx.doi.org/10.1021/sb4000959 | *ACS Synth. Biol.* 2014, 3, 152−162

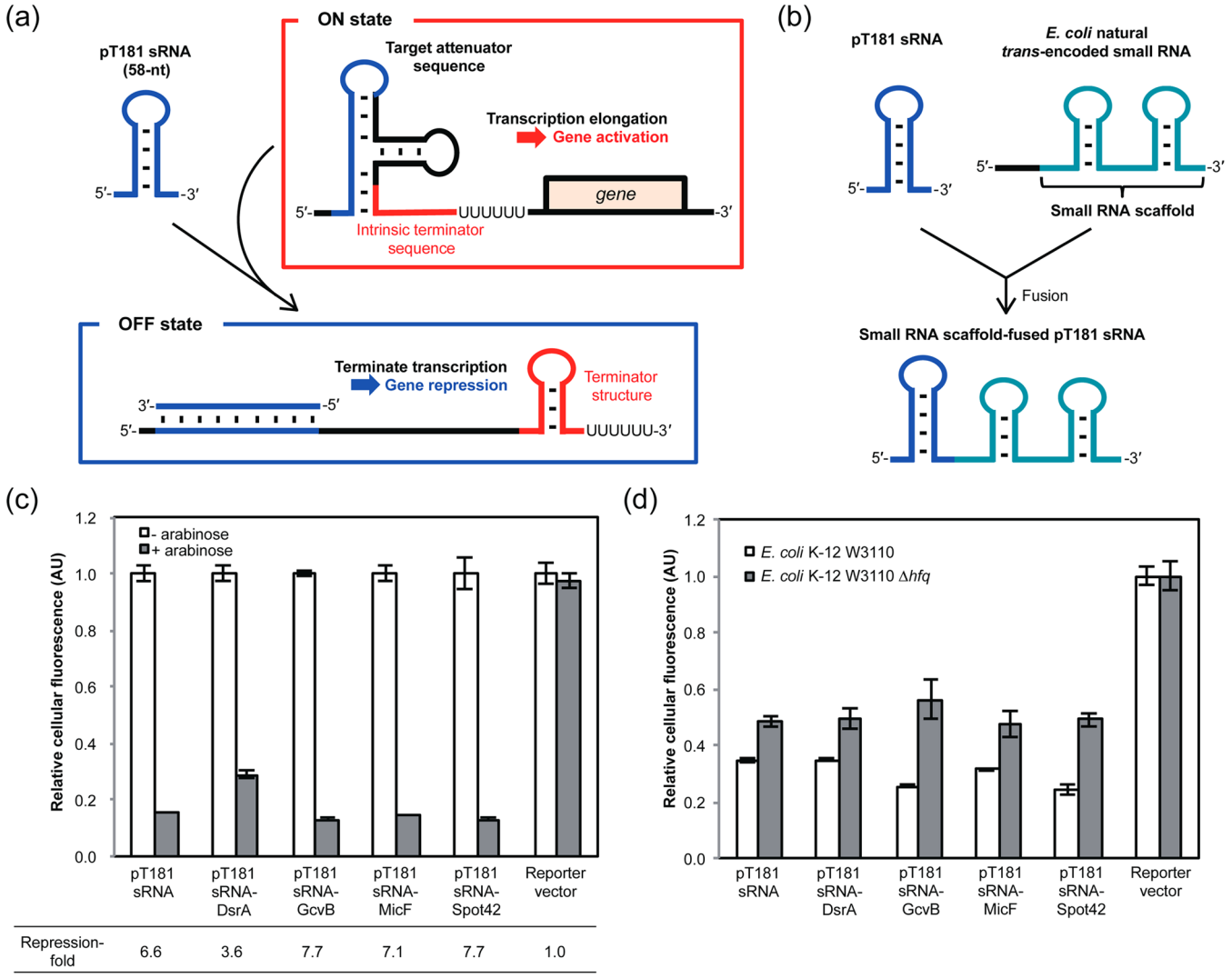

Figure 5. Target gene regulation mediated by pT181 sRNAs and the fusion of an sRNA scaffold. (a) pT181 sRNA was hybridized to the target attenuator sequence present in the 5′ UTR of the target mRNA to form a transcription terminator, resulting in gene repression. (b) sRNA scaffolds were directly fused to the 3′ end of pT181 sRNA. (c) sRNA-scaffold-fused pT181 sRNAs were regulated using arabinose-inducible promoter P_{araBAD} and evaluated by measuring the repression level of GFPuv downstream of the pT181 target attenuator sequence. The cellular fluorescence in the absence of L-arabinose was normalized to 1.0. The fold repression is shown. (d) Evaluation of scaffold-fused pT181 sRNAs in the *E. coli* K-12 W3110 and Δ*hfq* strains (*E. coli* K-12 W3110 Δ*hfq*). The pT181 sRNAs were transcribed constitutively by $P_{LlacO-1}$. The cellular fluorescence of the reporter vector was normalized to 1.0. The graphs depict the mean and error bars represent the standard deviation of experiments performed in triplicate.

(Supporting Information Figure S4), and starting with analysis of the secondary structure followed by verification of experimental gene regulation could be an effective method to select appropriate sRNA scaffolds for fusion to improve the efficiencies of specific sRNAs. Moreover, we introduced mutations that were predicted to stabilize secondary structure and found that they were effective at enhancing gene regulation.

Fusion of sRNA Scaffolds to the Transcriptional Attenuator and Their Improvement. Because the fusion of a MicF scaffold and the predicted stabilization of secondary structure enhanced the artificial riboregulator system, we tested our strategy using a different gene-regulatory system that functions by a different mechanism to investigate if it could also enhance gene regulation. As a target system to fuse the sRNA scaffolds, we selected the pT181 attenuator system, which is a naturally occurring sRNA-based gene-regulatory system with a mechanism to control the copy number of *Staphylococcus aureus* plasmid pT181 (Figure 5a).[50] Whereas the riboregulator is a post-transcriptional gene regulator, this pT181 attenuator system controls transcription and is controlled by a noncoding sRNA (pT181 sRNA), and its target attenuator sequence resides in the 5′ UTR of the target mRNA and forms a hairpin structure. The pT181 sRNA hybridizes with the target hairpin sequence by loop−loop interactions and promotes the formation of an intrinsic transcription terminator to terminate transcription. Without the pT181 sRNA, the terminator structure is sequestered in the attenuator sequence and prolongs transcription. Previously, the pT181 attenuator system was used as an RNA tool in synthetic biology to mutate the loop sequences of both pT181 sRNA and its target attenuator hairpin sequence to construct orthogonal pairs.[14] It has also been shown to enable ligand-specific regulation by incorporating an RNA aptamer into the pT181 sRNA and has been described in designing logic gates.[15] Meanwhile, it has not been reported that Hfq is required for this transcriptional attenuator. Here, the four scaffolds (DsrA, GcvB, MicF, and Spot42) were

dx.doi.org/10.1021/sb4000959 | ACS Synth. Biol. 2014, 3, 152−162

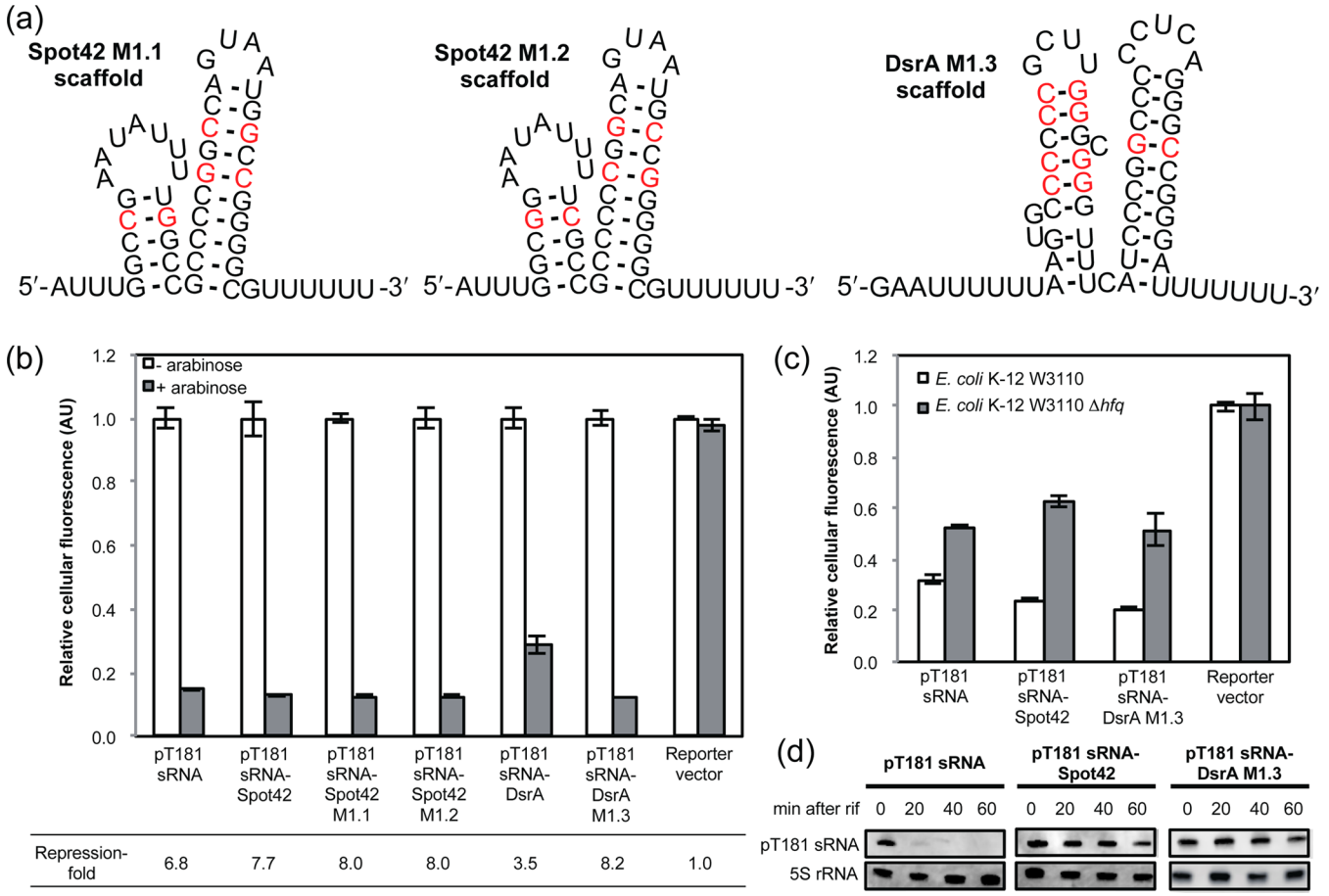

Figure 6. pT181 sRNA-Spot42 and pT181 sRNA-DsrA variants. (a) Spot42 and DsrA scaffold variants. Mutations predicted to stabilize the secondary structures were introduced into the hairpin structures. (b) Evaluation of the pT181 sRNA-Spot42 and pT181 sRNA-DsrA variants. The pT181 sRNA transcription was regulated using arabinose-inducible promoter P_{araBAD} and evaluated by measuring the repression level of GFPuv downstream of the pT181 target attenuator sequence. The cellular fluorescence in the absence of L-arabinose was normalized to 1.0. The fold repression is shown. (c) Evaluation of selected pT181 sRNAs in the *E. coli* K-12 W3110 and Δ*hfq* strains (*E. coli* K-12 W3110 Δ*hfq*). The pT181 sRNAs were transcribed constitutively by $P_{LlacO-1}$. The cellular fluorescence of the reporter vector was normalized to 1.0. (d) Northern blot analysis to confirm the stabilities of pT181 sRNA and scaffold-fused pT181 sRNAs. The strains were grown overnight at 37 °C in the presence of 0.1% L-arabinose. After incubation, rifampicin was added, and the cells were harvested at the indicated time points for RNA preparation. Total RNA was analyzed using probes specific for taR12 and 5S rRNA, respectively. The graphs depict the mean and error bars represent the standard deviation of experiments performed in triplicate.

directly fused to the 3′ end of pT181 sRNA consisting of a 58 nt antisense sequence,[15] and the transcription of scaffold-fused pT181 sRNAs was regulated by P_{araBAD} as described above (Figure 5b and Supporting Information Figure S3). Transcription attenuation was evaluated by measuring GFPuv fluorescence, which was encoded downstream of the target attenuator sequence under the control of a constitutive promoter. The fusion of three scaffolds (pT181 sRNA-GcvB, pT181 sRNA-MicF, and pT181 sRNA-Spot42) increased transcription attenuation, whereas fusion of the DsrA scaffold decreased the fold repression (Figure 5c). These enhancements in gene-regulation ability only were observed in cells expressing *hfq* but not in the Δ*hfq* strain (Figure 5d), demonstrating that the sRNA-scaffold-fused pT181 sRNAs were Hfq-dependent and that *hfq* was critical for higher gene-regulation abilities, as with the taRNAs described earlier.

For further improvement, mutations predicted to stabilize the Spot42 scaffold were introduced against Spot42-scaffold-fused pT181 sRNA (Figure 6a). The resulting two variants, pT181 sRNA-Spot42 M1.1 and pT181 sRNA-Spot42 M1.2, both slightly increased the repression (Figure 6b). Interestingly, the gene-regulation ability of pT181 sRNA-DsrA was dramatically improved by mutating the scaffold region (M1.3), which exhibited the highest fold repression of all sRNA-scaffold-fused pT181 sRNAs. Compared to pT181 sRNA, the pT181 sRNA-DsrA M1.3 did not improve gene-regulation ability in the *E. coli* K-12 W3110 Δ*hfq* strain (Figure 6c) and was shown to be more stable by northern blot analysis (Figure 6d), indicating fusion of sRNA scaffolds enabled Hfq binding. From these results, the fusion and engineering of sRNA scaffolds were also deemed effective against the transcriptional gene regulator pT181 sRNA that regulates target gene expression by a different mechanism from the riboregulator. Moreover, because the scaffolds that enhanced the gene-regulation abilities of taRNAs and pT181 sRNA were different, the scaffolds that improved the sRNA gene regulation ability were dependent on the sRNA sequence.

Substituting the Scaffold Region of the MicF sRNA into an Engineered MicF Scaffold. Stabilizing the secondary structures of the sRNA scaffolds enhanced the gene-regulation abilities of the post-transcriptional and transcriptional gene-regulatory systems. Therefore, we investigated whether

dx.doi.org/10.1021/sb4000959 | *ACS Synth. Biol.* 2014, 3, 152−162

stabilizing the secondary scaffold structure of naturally occurring *trans*-encoded sRNA would result in a similar improvement in gene regulation. To demonstrate our strategy, the MicF scaffold mutations (M3.1, M3.2, M4.3, and M7.4) that were able to enhance the gene-regulatory abilities of the taRNA-MicFs were introduced into the naturally occurring *E. coli* MicF sRNA, the origin of the MicF scaffold. This MicF sRNA repressed expression of the outer-membrane porin gene *ompF* through hybridization with a sequence including the RBS and start codon (Supporting Information Figure S12).[43] The *ompF* 5′ UTR and first 12 codons of the *ompF* coding region were cloned and fused to the *gfpuv* open reading frame as described previously.[19] The *ompF::gfpuv* genes were transcribed constitutively under the $P_{LtetO-1}$ promoter, and subsequent repression mediated by the MicF sRNA variants was evaluated by inducing their transcription from the P_{araBAD} promoter. As a result, the MicF sRNA M3.2 variant, harboring the stabilized downstream hairpin structure, repressed *ompF::gfpuv* 15-fold, which was approximately 1.9-fold higher than that of the mutation-free MicF sRNA (8.1-fold repression) (Figure 7). The M3.1 and M4.3 variants have mutations in the

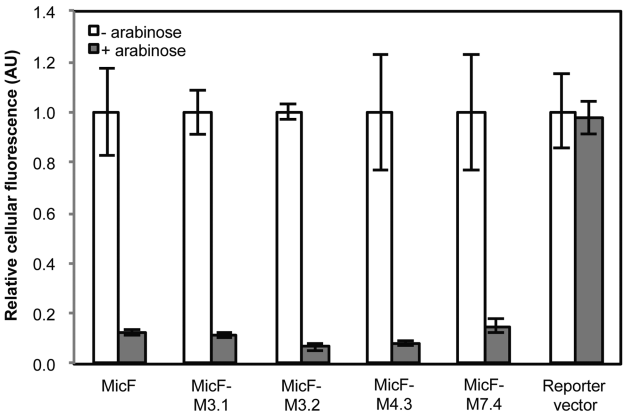

Figure 7. MicF sRNA variants targeting *ompF::gfpuv*. The mutations that improved taRNA gene regulation were introduced into MicF sRNA. MicF sRNA transcription was regulated using arabinose-inducible promoter P_{araBAD} and evaluated by measuring the repression of constitutively transcribed *ompF::gfpuv*. The cellular fluorescence in the absence of L-arabinose was normalized to 1.0. The fold repression is shown. The graphs depict the mean and error bars represent the standard deviation of experiments performed in triplicates.

upstream hairpin structures, resulting in a shortened antisense region of two bases that hybridize within the vicinity of the RBS in the *ompF* 5′-UTR (Supporting Information Figure S12). Despite the shorter antisense regions, the M3.1 and M4.3 variants increased the fold repression (8.9- and 12-fold, respectively), which demonstrated that the mutations that enhanced taRNA-MicF gene-regulation ability were also able to improve MicF sRNA gene regulation. However, the MicF sRNA M7.4 variant did not increase the fold repression of *ompF::gfpuv*; therefore, the loop-sequence substitution may have resulted in unexpected intramolecular interactions. Although MicF targets the *ompF* gene, additional MicF targets have been reported recently.[34] Corcoran et al. demonstrated that the 5′ region of MicF hybridizes and regulates *lpxR*, *yahO*, *bssS*, and *lrp*. Here, we engineered the scaffold region, although the antisense region remained intact. Because of the intact antisense region of MicF, the variants may also increase gene regulation of the additional target genes.

Conclusions. In the present study, we directly fused naturally occurring *E. coli trans*-encoded sRNA-derived sRNA scaffolds, which included Hfq-binding sequences and rho-independent transcription terminator sequences, to the 3′ end of the taRNA of the riboregulator system (Figure 1b) and pT181 sRNA of the transcriptional attenuator system (Figure 5b). The MicF scaffold fused to taR12 achieved the highest increase in the gene-expression level. To improve this system further, the MicF scaffold was mutated in a manner predicted to stabilize its secondary structure by substituting the AU base pairs present in the hairpin structures with GC base pairs, which increased its gene-expression ability (Figure 4a). Whereas, in pT181 sRNA of the transcriptional attenuator, the engineered DsrA scaffold fusion exhibited the highest gene-repression ability (Figure 6a). The scaffold-fused RNA gene regulators required *hfq* for gene regulation and demonstrated higher stabilities. The mutations introduced into the MicF scaffold that improved taRNA-MicF-mediated gene-expression abilities were also effective in improving MicF sRNA (Figure 7).

To the best of our knowledge, this is the first report to focus on sRNA scaffolds to improve gene regulation further. Our strategy can improve the function of sRNAs that regulate both post-transcriptional and transcriptional gene expression without affecting the background expression levels because we only engineered sRNAs and not mRNAs (herein, crRNA or target attenuator sequence). Stabilization of the secondary structures of sRNA scaffolds can be an effective approach for improving scaffold-fused sRNAs and Hfq-dependent *trans*-encoded sRNAs that contain sRNA scaffolds and presents a valuable strategy to engineer sRNAs that strongly regulate target gene expression.

METHODS

Materials. All oligonucleotides used in this research were obtained from Operon Biotechnologies, Inc. (Huntsville, AL, USA) and are listed in Supporting Information Table S1. All restriction enzymes were obtained from Fermentas (Vilnius, Lithuania). All BioBrick standard biological parts were obtained from the Registry of Standard Biological Parts (http://partsregistry.org).

Bacterial Strains. *E. coli* DH5α cells were used for plasmid construction, and *E. coli* TOP10F′ cells (Invitrogen; Carlsbad, CA, USA) were used to evaluate the constructs. *E. coli* K-12 W3110 (host strain) and *E. coli* K-12 W3110 Δ*hfq* (*hfq* deletion strain) were used to evaluate the selected sRNAs and were provided from Dr. Hiroji Aiba (Suzuka University of Medical Sciences, Suzuka, Japan).[47]

Plasmids Construction. All constructed plasmids are listed in Supporting Information Table S2. GFPuv (Clontech; Mountain View, CA, USA) was used to evaluate each taRNA, pT181 sRNA, and sRNA. The following were obtained from the BioBricks Foundation's Registry of Standard Biological Parts: P_{araBAD}/*araC* (BBa_I0500), constitutive promoter (BBa_J23119), double terminator (BBa_B0015), and high-copy-vectors pSB1K3 and pSB1A2.

Riboregulators were constructed as described previously.[10,13] The sRNA scaffold[18] of four naturally occurring *E. coli trans*-encoded sRNAs (DsrA, GcvB, MicF, and Spot42) were cloned from *E. coli* K-12 genomic DNA using gene-specific primers. Each scaffold was directly fused to the 3′ end of taR12 and taR*2 by digestion with restriction enzymes *Nhe*I and *Sac*I.

dx.doi.org/10.1021/sb4000959 | *ACS Synth. Biol.* 2014, 3, 152−162

Arabinose-inducible promoter $P_{araBAD}/araC$ was used to control taRNA transcription, and isopropyl β-D-1-thiogalactopyranoside (IPTG)-inducible $P_{LlacO-1}$[9] was used to control crRNA transcription except in the experiment to evaluate the expression efficiency in which $P_{araBAD}/araC$ was used to control the transcription of both taRNA and crRNA. The GFPuv and double terminator were ligated by 3A assembly and inserted downstream of crRNA by digestion with the restriction enzymes *Kpn*I and *Pst*I. The taRNA and crRNA cassettes were ligated and inserted into the high-copy-vector pSB1K3 (Registry of Standard Biological Parts). To construct the constitutively transcribing taRNA plasmids, the $P_{LtetO-1}$ promoter and high-copy pSB1A2 vector were used instead of $P_{araBAD}/araC$ and pSB1K3, respectively.

The attenuator[14,15] was synthetized by FASMAC Co., Ltd. (Kanagawa, Japan), and MicF scaffolds were directly fused to the 3′ end of pT181 sRNA, as described above, by digestion with *Nhe*I and *Sac*I. The pT181 target sequence was inserted into the mid-copy-number plasmid pSTV28 (Takara Bio Inc.; Shiga, Japan) under a constitutive promoter (BBa_J23119; Registry of Standard Biological Parts), and the GFPuv double terminator was inserted downstream of the target attenuator sequence. For the RBS, the RBS-S sequence[14] was used. To construct a plasmid that constitutively transcribes pT181 sRNA, the $P_{LlacO-1}$ promoter and the high-copy-number pSB1A2 vector were used instead of $P_{araBAD}/araC$ and pSB1K3, respectively.

All MicF scaffold variants were designed using M-fold secondary-structure prediction[38] to ensure that the mutations did not alter the secondary structures. MicF sRNA and taRNA-MicF variants were constructed by performing inverse PCR with the gene-specific primers listed in Supporting Information Table S1. All constructed plasmids were confirmed by sequencing.

The MicF sRNA, the 5′ UTR, and the first 12 codons of the coding region (leader sequence) of the target gene *ompF* were cloned from *E. coli* K-12 genomic DNA using the designated primers. The GFPuv open reading frame was fused to the *ompF* leader sequence as described previously.[19] MicF sRNA transcription was controlled using the $P_{araBAD}/araC$ and *ompF::gfpuv* by $P_{LtetO-1}$.[9] Both constructs contained transcriptional double terminators and were ligated and inserted into the high-copy-vector pSB1K3.

GFPuv Assay. Single colonies of *E. coli* TOP10F′ cells transformed with the intended plasmids were inoculated into 1 mL of LB medium containing appropriate antibiotics and cultured overnight at 37 °C. IPTG was added to the medium at a final concentration of 1 mM when evaluating riboregulators, and to induce taRNA, pT181 sRNA, or MicF sRNA transcription, L-arabinose was added to the medium at a final concentration of 0.1% (w/v). After 15 h of incubation, cells from 500 μL of the culture were harvested by centrifugation (4500*g*, 10 min), washed by resuspending in 240 μL of phosphate-buffered saline (PBS; 137 mM NaCl, 2.7 mM KCl, 8.1 mM Na_2HPO_4, and 1.47 mM KH_2PO_4, pH 7.4), recentrifuged, and resuspended in 240 μL of PBS, of which 200 μL was transferred to a 96-well microtiter plate. GFPuv fluorescence and optical density at 595 nm were measured using a multilabel plate counter (Wallac 1420 ARVO MX, PerkinElmer; Waltham, MA, USA; Ex: 390 nm/20 nm, Em: 520 nm/20 nm). The GFPuv fluorescence was normalized with the values of cell growth (OD_{595}) to calculate cellular fluorescence and to evaluate the taRNA, pT181 sRNA, or MicF sRNA.

To evaluate taRNAs and pT181 sRNAs in *E. coli* K-12 W3110 (host strain) and *E. coli* K-12 W3110 Δ*hfq* (*hfq* deletion strain), both strains were transformed with the intended plasmids, and single colonies were inoculated into 1 mL of LB medium containing appropriate antibiotics, cultured overnight at 37 °C, and evaluated by measuring GFPuv fluorescence and optical density at 595 nm as described above.

Northern Blot Analysis. Total RNAs were purified using NucleoSpin RNA II (TaKaRa Bio Inc.; Shiga, Japan) from rifampicin (500 μg/mL)-treated cells according to the manufacturer's instructions. Total RNA (4−10 μg) was denatured for 5 min at 95 °C, separated on 10% TBE-urea gels, and transferred onto nylon membranes (iBlot DNA transfer stacks; Invitrogen) using the iBlot Gel transfer device (Invitrogen). To detect taR12, pT181 sRNA, and 5S rRNA, 5′-biotinylated DNA probes[51] (Supporting Information Table S1) were used and hybridized for 16 h at 42 °C in 5× saline sodium citrate (SSC)/1% sodium dodecyl sulfate (SDS). The membranes were washed with 2× SSC/0.1% SDS (room temperature), 2× SSC/0.1% SDS (42 °C), and 1× SSC/0.1% SDS (42 °C) for 10 min each. After blocking with 2% bovine serum albumin in 5× SSC/1% SDS for 30 min at room temperature, the membranes were incubated with horseradish peroxidase-conjugated NeutrAvidin (Thermo Scientific; Rockford, IL, USA) in 5× SSC/1% SDS for 30 min at room temperature, visualized with Immobilon western chemiluminescent HRP substrate (Millipore; Billerica, MA, USA), and detected using the ImageQuant LAS 4000 mini system (GE Healthcare; Munich, Germany).

■ ASSOCIATED CONTENT

Supporting Information

This material is available free of charge via the Internet at http://pubs.acs.org.

■ AUTHOR INFORMATION

Corresponding Author

*Tel/Fax: + 81-42-388-7030. E-mail: ikebu@cc.tuat.ac.jp.

Present Address

§School of Bioscience and Biotechnology, Tokyo University of Technology, 1404-1 Katakuramachi, Hachioji, Tokyo 192-0982, Japan.

Notes

The authors declare no competing financial interest.

■ ACKNOWLEDGMENTS

This study was supported financially by the Core Research of Evolutional Science & Technology program (CREST) from the Japan Science and Technology Agency (JST). We thank Dr. Hiroji Aiba (Suzuka University of Medical Sciences, Suzuka, Japan) for providing the *E. coli* K-12 W3110 (IT1568) and *E. coli* K-12 W3110 Δ*hfq* (TM589) strains.

■ ABBREVIATIONS

IPTG, isopropyl β-D-1-thiogalactopyranoside; crRNA, *cis*-repressed mRNA; RBS, ribosomal binding site; SDS, sodium dodecyl sulfate; sRNA, small RNA; SSC, saline sodium citrate; taRNA, *trans*-activating noncoding RNA; UTR, untranslated region

REFERENCES

(1) Salis, H. M., Mirsky, E. A., and Voigt, C. A. (2009) Automated design of synthetic ribosome binding sites to control protein expression. *Nat. Biotechnol. 27*, 946−950.

(2) Callura, J. M., Dwyer, D. J., Isaacs, F. J., Cantor, C. R., and Collins, J. J. (2010) Tracking, tuning, and terminating microbial physiology using synthetic riboregulators. *Proc. Natl. Acad. Sci. U.S.A. 107*, 15898−15903.

(3) Zhang, F., Carothers, J. M., and Keasling, J. D. (2012) Design of a dynamic sensor-regulator system for production of chemicals and fuels derived from fatty acids. *Nat. Biotechnol. 30*, 354−359.

(4) Chen, S., Zhang, H., Shi, H., Ji, W., Feng, J., Gong, Y., Yang, Z., and Ouyang, Q. (2012) Automated design of genetic toggle switches with predetermined bistability. *ACS Synth. Biol. 1*, 284−290.

(5) Pfleger, B. F., Pitera, D. J., Smolke, C. D., and Keasling, J. D. (2006) Combinatorial engineering of intergenic regions in operons tunes expression of multiple genes. *Nat. Biotechnol. 24*, 1027−1032.

(6) Yokobayashi, Y., Weiss, R., and Arnold, F. H. (2002) Directed evolution of a genetic circuit. *Proc. Natl. Acad. Sci. U.S.A. 99*, 16587−16591.

(7) Brewster, R. C., Jones, D. L., and Phillips, R. (2012) Tuning promoter strength through RNA polymerase binding site design in *Escherichia coli*. *PLoS Comput. Biol. 8*, e1002811-1−e1002811-10.

(8) Blazeck, J., Garg, R., Reed, B., and Alper, H. S. (2012) Controlling promoter strength and regulation in *Saccharomyces cerevisiae* using synthetic hybrid promoters. *Biotechnol. Bioeng. 109*, 2884−2895.

(9) Lutz, R., and Bujard, H. (1997) Independent and tight regulation of transcriptional units in *Escherichia coli* via the LacR/O, the TetR/O and AraC/I1-I2 regulatory elements. *Nucleic Acids Res. 25*, 1203−1210.

(10) Isaacs, F. J., Dwyer, D. J., Ding, C., Pervouchine, D. D., Cantor, C. R., and Collins, J. J. (2004) Engineered riboregulators enable post-transcriptional control of gene expression. *Nat. Biotechnol. 22*, 841−847.

(11) Callura, J. M., Cantor, C. R., and Collins, J. J. (2012) Genetic switchboard for synthetic biology applications. *Proc. Natl. Acad. Sci. U.S.A. 109*, 5850−5855.

(12) Rodrigo, G., Landrain, T. E., and Jaramillo, A. (2012) *De novo* automated design of small RNA circuits for engineering synthetic riboregulation in living cells. *Proc. Natl. Acad. Sci. U.S.A. 109*, 15271−15276.

(13) Abe, K., Sakai, Y., Nakashima, S., Araki, M., Yoshida, W., Sode, K., Ikebukuro, K. (2013) Design of riboregulators for control of cyanobacterial (*Synechocystis*) protein expression. *Biotechnol. Lett.* [Online early access]. DOI: 10.1007/s10529-013-1352-x. Published Online: Sept 2013.

(14) Lucks, J. B., Qi, L., Mutalik, V. K., Wang, D., and Arkin, A. P. (2011) Versatile RNA-sensing transcriptional regulators for engineering genetic networks. *Proc. Natl. Acad. Sci. U.S.A. 108*, 8617−8622.

(15) Qi, L., Lucks, J. B., Liu, C. C., Mutalik, V. K., and Arkin, A. P. (2012) Engineering naturally occurring *trans*-acting non-coding RNAs to sense molecular signals. *Nucleic Acids Res. 40*, 5775−5786.

(16) Takahashi, M. K., and Lucks, J. B. (2013) A modular strategy for engineering orthogonal chimeric RNA transcription regulators. *Nucleic Acids Res. 41*, 7577−7588.

(17) Man, S., Cheng, R., Miao, C., Gong, Q., Gu, Y., Lu, X., Han, F., and Yu, W. (2011) Artificial *trans*-encoded small non-coding RNAs specifically silence the selected gene expression in bacteria. *Nucleic Acids Res. 39*, e50.

(18) Sharma, V., Nomura, Y., and Yokobayashi, Y. (2008) Engineering complex riboswitch regulation by dual genetic selection. *J. Am. Chem. Soc. 130*, 16310−16315.

(19) Sharma, V., Yamamura, A., and Yokobayashi, Y. (2012) Engineering artificial small RNAs for conditional gene silencing in *Escherichia coli*. *ACS Synth Biol 1*, 6−13.

(20) Sharma, V., Sakai, Y., Smythe, K. A., and Yokobayashi, Y. (2013) Knockdown of *recA* gene expression by artificial small RNAs in *Escherichia coli*. *Biochem. Biophys. Res. Commun. 430*, 256−259.

(21) Na, D., Yoo, S. M., Chung, H., Park, H., Park, J. H., and Lee, S. Y. (2013) Metabolic engineering of *Escherichia coli* using synthetic small regulatory RNAs. *Nat. Biotechnol. 31*, 170−174.

(22) Nakashima, N., Tamura, T., and Good, L. (2006) Paired termini stabilize antisense RNAs and enhance conditional gene silencing in *Escherichia coli*. *Nucleic Acids Res. 34*, e138.

(23) Nakashima, N., and Tamura, T. (2009) Conditional gene silencing of multiple genes with antisense RNAs and generation of a mutator strain of *Escherichia coli*. *Nucleic Acids Res. 37*, e103.

(24) Zhang, A., Altuvia, S., Tiwari, A., Argaman, L., Hengge-Aronis, R., and Storz, G. (1998) The OxyS regulatory RNA represses *rpoS* translation and binds the Hfq (HF-I) protein. *EMBO J. 17*, 6061−6068.

(25) Majdalani, N., Cunning, C., Sledjeski, D., Elliott, T., and Gottesman, S. (1998) DsrA RNA regulates translation of RpoS message by an anti-antisense mechanism, independent of its action as an antisilencer of transcription. *Proc. Natl. Acad. Sci. U.S.A. 95*, 12462−12467.

(26) Raghavan, R., Groisman, E. A., and Ochman, H. (2011) Genome-wide detection of novel regulatory RNAs in *E. coli*. *Genome Res. 21*, 1487−1497.

(27) Zhang, A., Wassarman, K. M., Rosenow, C., Tjaden, B. C., Storz, G., and Gottesman, S. (2003) Global analysis of small RNA and mRNA targets of Hfq. *Mol. Microbiol. 50*, 1111−1124.

(28) Wassarman, K. M., Repoila, F., Rosenow, C., Storz, G., and Gottesman, S. (2001) Identification of novel small RNAs using comparative genomics and microarrays. *Genes Dev. 15*, 1637−1651.

(29) Masse, E., Escorcia, F. E., and Gottesman, S. (2003) Coupled degradation of a small regulatory RNA and its mRNA targets in *Escherichia coli*. *Genes Dev. 17*, 2374−2383.

(30) Moller, T., Franch, T., Udesen, C., Gerdes, K., and Valentin-Hansen, P. (2002) Spot 42 RNA mediates discoordinate expression of the *E. coli* galactose operon. *Genes Dev. 16*, 1696−1706.

(31) Papenfort, K., Sun, Y., Miyakoshi, M., Vanderpool, C. K., and Vogel, J. (2013) Small RNA-mediated activation of sugar phosphatase mRNA regulates glucose homeostasis. *Cell 153*, 426−437.

(32) Pfeiffer, V., Papenfort, K., Lucchini, S., Hinton, J. C., and Vogel, J. (2009) Coding sequence targeting by MicC RNA reveals bacterial mRNA silencing downstream of translational initiation. *Nature Struct. Mol. Biol. 16*, 840−846.

(33) Opdyke, J. A., Kang, J. G., and Storz, G. (2004) GadY, a small-RNA regulator of acid response genes in *Escherichia coli*. *J. Bacteriol. 186*, 6698−6705.

(34) Corcoran, C. P., Podkaminski, D., Papenfort, K., Urban, J. H., Hinton, J. C., and Vogel, J. (2012) Superfolder GFP reporters validate diverse new mRNA targets of the classic porin regulator, MicF RNA. *Mol. Microbiol. 84*, 428−445.

(35) Papenfort, K., Bouvier, M., Mika, F., Sharma, C. M., and Vogel, J. (2010) Evidence for an autonomous 5′ target recognition domain in an Hfq-associated small RNA. *Proc. Natl. Acad. Sci. U.S.A. 107*, 20435−20440.

(36) Sledjeski, D. D., Whitman, C., and Zhang, A. (2001) Hfq is necessary for regulation by the untranslated RNA DsrA. *J. Bacteriol. 183*, 1997−2005.

(37) Moller, T., Franch, T., Hojrup, P., Keene, D. R., Bachinger, H. P., Brennan, R. G., and Valentin-Hansen, P. (2002) Hfq: Abacterial Sm-like protein that mediates RNA-RNA interaction. *Mol. Cell 9*, 23−30.

(38) Zhang, A., Wassarman, K. M., Ortega, J., Steven, A. C., and Storz, G. (2002) The Sm-like Hfq protein increases OxyS RNA interaction with target mRNAs. *Mol. Cell 9*, 11−22.

(39) Urban, J. H., and Vogel, J. (2007) Translational control and target recognition by *Escherichia coli* small RNAs *in vivo*. *Nucleic Acids Res. 35*, 1018−1037.

(40) Vogel, J., and Luisi, B. F. (2011) Hfq and its constellation of RNA. *Nat. Rev. Microbiol. 9*, 578−589.

(41) Brescia, C. C., Mikulecky, P. J., Feig, A. L., and Sledjeski, D. D. (2003) Identification of the Hfq-binding site on DsrA RNA: Hfq binds without altering DsrA secondary structure. *RNA 9*, 33−43.

(42) Zuker, M. (2003) Mfold web server for nucleic acid folding and hybridization prediction. *Nucleic Acids Res. 31*, 3406−3415.
(43) Delihas, N., and Forst, S. (2001) MicF: An antisense RNA gene involved in response of *Escherichia coli* to global stress factors. *J. Mol. Biol. 313*, 1−12.
(44) Franch, T., Petersen, M., Wagner, E. G., Jacobsen, J. P., and Gerdes, K. (1999) Antisense RNA regulation in prokaryotes: Rapid RNA/RNA interaction facilitated by a general U-turn loop structure. *J. Mol. Biol. 294*, 1115−1125.
(45) Sledjeski, D. D., Gupta, A., and Gottesman, S. (1996) The small RNA, DsrA, is essential for the low temperature expression of RpoS during exponential growth in *Escherichia coli*. *EMBO J. 15*, 3993−4000.
(46) Urbanowski, M. L., Stauffer, L. T., and Stauffer, G. V. (2000) The *gcvB* gene encodes a small untranslated RNA involved in expression of the dipeptide and oligopeptide transport systems in *Escherichia coli*. *Mol. Microbiol. 37*, 856−868.
(47) Morita, T., Maki, K., and Aiba, H. (2005) RNase E-based ribonucleoprotein complexes: Mechanical basis of mRNA destabilization mediated by bacterial noncoding RNAs. *Genes Dev. 19*, 2176−2186.
(48) Lorenz, C., Gesell, T., Zimmermann, B., Schoeberl, U., Bilusic, I., Rajkowitsch, L., Waldsich, C., von Haeseler, A., and Schroeder, R. (2010) Genomic SELEX for Hfq-binding RNAs identifies genomic aptamers predominantly in antisense transcripts. *Nucleic Acids Res. 38*, 3794−3808.
(49) Link, T. M., Valentin-Hansen, P., and Brennan, R. G. (2009) Structure of *Escherichia coli* Hfq bound to polyriboadenylate RNA. *Proc. Natl. Acad. Sci. U.S.A. 106*, 19292−19297.
(50) Kumar, C. C., and Novick, R. P. (1985) Plasmid pT181 replication is regulated by two countertranscripts. *Proc. Natl. Acad. Sci. U.S.A. 82*, 638−642.
(51) Masse, E., Vanderpool, C. K., and Gottesman, S. (2005) Effect of RyhB small RNA on global iron use in *Escherichia coli*. *J. Bacteriol. 187*, 6962−6971.